hnRNP U protein is required for normal pre-mRNA splicing and postnatal heart development and function

Junqiang Ye[a], Nadine Beetz[b,c], Sean O'Keeffe[a], Juan Carlos Tapia[a], Lindsey Macpherson[a], Weisheng V. Chen[a], Rhonda Bassel-Duby[b], Eric N. Olson[b], and Tom Maniatis[a,1]

[a]Department of Biochemistry and Molecular Biophysics, Columbia University College of Physicians and Surgeons, New York, NY 10032; [b]Department of Molecular Biology, University of Texas Southwestern Medical Center, Dallas, TX 75390; and [c]Institute of Experimental and Clinical Pharmacology and Toxicology, University of Freiburg, 79104 Freiburg, Germany

Contributed by Tom Maniatis, April 30, 2015 (sent for review March 2, 2015; reviewed by Brenton R. Graveley)

We report that mice lacking the heterogeneous nuclear ribonucleoprotein U (hnRNP U) in the heart develop lethal dilated cardiomyopathy and display numerous defects in cardiac pre-mRNA splicing. Mutant hearts have disorganized cardiomyocytes, impaired contractility, and abnormal excitation–contraction coupling activities. RNA-seq analyses of *Hnrnpu* mutant hearts revealed extensive defects in alternative splicing of pre-mRNAs encoding proteins known to be critical for normal heart development and function, including *Titin* and calcium/calmodulin-dependent protein kinase II delta (*Camk2d*). Loss of hnRNP U expression in cardiomyocytes also leads to aberrant splicing of the pre-mRNA encoding the excitation–contraction coupling component Junctin. We found that the protein product of an alternatively spliced Junctin isoform is *N*-glycosylated at a specific asparagine site that is required for interactions with specific protein partners. Our findings provide conclusive evidence for the essential role of hnRNP U in heart development and function and in the regulation of alternative splicing.

heart development | alternative splicing | RNA-seq | dilated cardiomyopathy | *N*-glycosylation

The expression of more than 95% of human genes is affected by alternative pre-mRNA splicing (AS) (1, 2). Differentially spliced isoforms play distinct roles in a temporally and spatially specific manner (3), and mutations that lead to aberrant splicing are the cause of many human genetic diseases (4). RNA-binding proteins (RBPs) play a central role in the regulation of alternative splicing during development and disease. They function primarily by positively or negatively regulating splice-site recognition by the spliceosome (1). Many RBPs are expressed in specific tissues, and AS is regulated by the combinatorial activities of these factors on specific pre-mRNAs through their interactions with distinct regulatory sequences in pre-mRNA that function as splicing enhancers or silencers (5).

The developing heart is one of the best studied systems where splicing changes occur during normal development, and mutations affecting specific splicing outcomes contribute to cardiomyopathy (6, 7). Although these mutations can either disrupt splicing elements or affect the expression of specific splicing factors, the latter mechanism is clearly responsible for the distinct splicing profiles at different developmental stages. For example, the dynamics of alternative splicing during postnatal heart development correlate with expression changes of many RBPs, including CUG-BP, Elav-like family member 1 (CELF1), Muscleblind-like 1 (MBNL1), and FOX proteins (8). Detailed biochemical studies have elucidated the mechanisms by which these splicing factors regulate splicing in a position- and context-dependent manner (9, 10). The function of other RBPs during heart development has also been studied. For example, two of the muscle-specific splicing factors, RBM20 and RBM24, play distinct roles in splicing regulation. RBM20 mainly acts as a splicing repressor, as its absence leads to multiple exon inclusion events in the heart. For example, the *Titin* gene is one of the major targets of RBM20 (11, 12). On the other hand, loss of RBM24 expression gives rise to many exon skipping events (13), implicating RBM24 as a splicing activator. Strikingly, there is little overlap between RBM20 and RBM24 splicing targets, suggesting that RBM20 and RBM24 are involved in regulating splicing of distinct groups of pre-mRNAs and there is little cross-talk between these two splicing factors.

Distinct splicing activities have also been ascribed to general splicing factors (1). There are two major types of ubiquitously expressed RBPs: the heterogeneous nuclear ribonucleoproteins (hnRNPs) and serine/arginine (SR)-rich proteins. hnRNPs and SR proteins are generally believed to play opposite roles in splicing: SR proteins promote the inclusion of exons during splicing, whereas hnRNP proteins repress inclusion (1). The function of certain SR proteins has been studied in the mouse heart through the conditional knockout approach. *Srsf1* deletion in the heart leads to lethal dilated cardiomyopathy (DCM) (death occurs 6–8 wk after birth) (14). SRSF1 is required for the cardiac-specific splicing of *Cypher* (also called *Ldb3*) pre-mRNA, and the regulation of alternative splicing of calcium/calmodulin-dependent protein kinase II delta (*Camk2d*) and cardiac *Troponin T* (*cTnT*) during heart development. In particular, the persistent splicing of a neuronal isoform of *Camk2d* and its ability to enhance excitation and contraction coupling (ECC) activity in *Srsf1* mutant cardiomyocytes have been proposed as a possible cause of the phenotype in mutant mice (14). Ablation of another SR protein, SRSF10 (SRp38), from the mouse also leads to heart defects (15). SRSF10 has been shown to regulate the splicing of Triadin, an important component of ECC machinery (15). Interestingly, conditional deletion of *Srsf2* from the heart leads to DCM with little splicing misregulation but instead affects the expression of

Significance

We studied the physiological function of the heterogeneous nuclear ribonucleoprotein U (hnRNP U) by generating a conditional knockout mouse in which the *Hnrnpu* gene is deleted in the heart. We found that hnRNP U is required for normal pre-mRNA splicing and postnatal heart development and function. Mutant mice develop severe dilated cardiomyopathy and die 2 wk after birth. Phenotypic characterization of mutant hearts coupled with RNA-seq data analyses revealed that mutant hearts display multiple cardiac defects as a result of misregulated gene expression and abnormal pre-mRNA splicing. We also identified the sarcoplasmic reticulum membrane protein Junctin as a splicing target of hnRNP U and provide an interesting example of alternative splicing in controlling the modification and function of proteins.

Author contributions: J.Y., E.N.O., and T.M. designed research; J.Y., N.B., J.C.T., L.M., and W.V.C. performed research; J.Y., N.B., S.O., L.M., R.B.-D., E.N.O., and T.M. analyzed data; and J.Y. and T.M. wrote the paper.

Reviewers included: B.R.G., University of Connecticut Health Center.

The authors declare no conflict of interest.

Data deposition: The data reported in this paper have been deposited in the Gene Expression Omnibus (GEO) database, www.ncbi.nlm.nih.gov/geo (accession no. GSE68178).

[1]To whom correspondence should be addressed. Email: tm2472@columbia.edu.

This article contains supporting information online at www.pnas.org/lookup/suppl/doi:10.1073/pnas.1508461112/-/DCSupplemental.

the calcium channel Ryr2 (16). It is striking that these SR proteins affect ECC activity in the heart by directly regulating the expression/splicing of distinct players in this machinery. Because these studies were conducted before the advent of next-generation RNA sequencing, only a few splicing targets specifically regulated by these SR proteins were identified. A more comprehensive study of the effects of deleting the genes encoding these proteins from the heart on the splicing program has not been reported.

In contrast to SR proteins, specific functions of hnRNP proteins in cardiac pre-mRNA splicing have not been determined. In this report, we selectively inactivated the expression of one of the most abundant hnRNP proteins—hnRNP U—in the heart. We found that *Hnrnpu* mutant mice develop a lethal DCM phenotype, with death occurring around 2 wk after birth. There are multiple cardiac defects in mutant hearts accompanied by many splicing alterations. Some of these splicing targets are commonly regulated by hnRNP U and other SR and RBM proteins. We also identified many hnRNP U-specific splicing targets in the heart, including an ECC component Junctin. The protein product of the alternatively spliced Junctin isoform is *N*-glycosylated at a specific asparagine site in *Hnrnpu* mutant cells and could contribute to abnormal cardiac function. Our study also enables comparisons of the roles of different splicing factors in heart development and function.

Results

Generation of an *Hnrnpu* Conditional Knockout Mouse Line. hnRNP U is the highest molecular weight (MW) protein in the hnRNP complex and is one of the most abundant and ubiquitously expressed hnRNP proteins (17, 18). hnRNP U, which binds to both RNA and DNA, is thought to play a central role in transcription, RNA processing, and nuclear organization (17, 19, 20). Recently, hnRNP U has been shown to bind specifically to long noncoding RNAs (lncRNAs) and play a role in chromosome organization. For example, hnRNP U is required for normal X chromosome inactivation (21) and for the maintenance of specific nuclear interchromosomal conformation mediated by lncRNA Firre (22). hnRNP U has also been shown to play an important role in splicing regulation in cultured cells (23, 24). However, different changes in splicing were observed in two studies in which hnRNP U was knocked down in cells in culture. In one study, knocking down hnRNP U expression was reported to result in comparable levels of exon inclusion and skipping events (23), whereas in another study hnRNP U was reported to preferentially promote exon inclusion (24).

Here we report a study of hnRNP U function in mice. We generated a conditional deletion allele of the mouse *Hnrnpu* gene by homologous recombination in mouse ES cells. Two loxP sites were engineered to flank a region of *Hnrnpu* genomic DNA encoding exons 4–14 (Fig. 1*A*). The insertion of these sites does not affect the normal processing of the *Hnrnpu* gene, as mice homozygous for the conditional allele are phenotypically indistinguishable from wild-type controls. Tissue-specific Cre-recombinase (Cre)-mediated deletion removes more than 65% of the hnRNP U coding sequence, which includes the conserved SPRY (involved in protein–protein interactions) and the RNA-binding RGG domains at the C terminus (25). The remaining N-terminal transcript after the deletion can give rise to a truncated hnRNP U protein devoid of RNA-binding activity. Breeding the *Hnrnpu* conditional line with a number of Cre lines demonstrated that hnRNP U expression can be efficiently reduced in targeted tissues (Fig. 1 *B* and *C*). We also generated a constitutive *Hnrnpu* mutant allele by crossing the conditional knockout mice with a germ-line–expressing *Sox2*-Cre line. Consistent with a report that hnRNP U is essential for mouse embryonic development (26), we failed to recover mice homozygous for the *Hnrnpu* mutant allele.

Deletion of the *Hnrnpu* Gene from the Heart Leads to a Sudden Death Phenotype. The *Hnrnpu* gene is expressed during all developmental stages of the mouse heart (Fig. S1). However, the level of hnRNP U expression gradually decreases from the embryonic and early postnatal stage to adulthood (Fig. S1). To study the role of hnRNP U in heart development and function, we crossed the conditional *Hnrnpu* knockout line with a cardiomyocyte-expressing Cre line, muscle creatine kinase-Cre (*Ckmm*-Cre), which is also active in skeletal muscle (*Ckmm*-Cre expression starts at E17.5 and continues to adulthood) (27). The conditional *Hnrnpu* knockout mice were born at the expected Mendelian ratio with no apparent abnormalities. Western blot analysis showed that full-length hnRNP U protein is expressed at a significantly reduced level in mutant hearts (Fig. 1*C*; greater than 80% reduction at P10 and P12). We used *Hnrnpu* f/f, *Ckmm*-Cre+ mice as mutants (Ckmm-KO) and *Hnrnpu* f/f, *Ckmm*-Cre–, or mice containing wild-type *Hnrnpu* allele as controls in this study. Residual levels of hnRNP U are most likely due to expression in noncardiomyocytes in the heart. Deletion of *Hnrnpu* from the heart is confirmed by immunofluorescence staining of heart sections with antibodies that recognize C-terminal hnRNP U (Fig. S2*B*). However, using antibodies that specifically recognize an N-terminal sequence of hnRNP U, we detected a lower MW protein band exclusively in mutant samples by Western blot analysis (Fig. S2*C*). Immunofluorescence staining with the same antibody also revealed the expression of the protein in both wild-type and mutant cardiomyocytes (Fig. S2*B*). Thus, we confirmed the existence of a truncated hnRNP U protein in our *Hnrnpu* mutant cells. The truncated protein of hnRNP U lacking SPRY and RGG domains can still interact with chromatin/DNA (through the N-terminal SAP domain) but not RNA (28). This mutant mouse line can thus be used to study the specific effects of eliminating hnRNP U–RNA interactions in vivo.

Although mutant animals appear morphologically indistinguishable from control littermates, they all die abruptly from heart failure around 14 d after birth. To examine the pathology in detail, hearts were dissected from surviving animals of different ages and subjected to hematoxylin and eosin (H&E) staining. We observed increased dilation of the ventricle chambers of the mutant hearts over time (dilation of the left ventricle chamber can be observed as early as P7). One example of H&E-stained sections of P14 hearts is presented in Fig. 2*A*. This staining clearly shows significantly enlarged ventricle chambers accompanied with thinning of the ventricle wall and septum. These are morphological features observed in mouse models with heart failure and characteristic of human patients with DCM (29). Thus, deletion of hnRNP U in the mouse heart leads to a lethal DCM phenotype, similar to that observed with deletion of the *Srsf1* gene in heart cells. However,

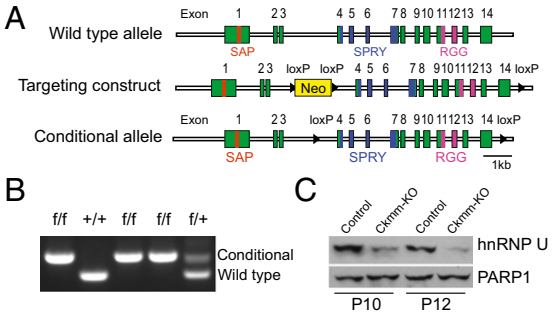

Fig. 1. Generation of an *Hnrnpu* conditional deletion allele. (*A*) Diagram of the gene targeting strategy. A triple loxP targeting construct was engineered for homologous recombination in ES cells. Correctly targeted ES cells were transfected with a Cre-recombinase–expressing plasmid to selectively remove the Neo cassette. Domains of hnRNP U encoded by different exons are also diagrammed. (*B*) An example of the characterization of the genotype of the *Hnrnpu* targeted allele. f, conditional allele; +, wild-type allele. (*C*) Conditional deletion of the *Hnrnpu* gene from the heart. Shown are Western blots for hnRNP U and PARP1 in heart protein lysates from control (*Hnrnpu* f/f; *Ckmm*-Cre–) and mutant (Ckmm-KO, *Hnrnpu* f/f; *Ckmm*-Cre+) animals.

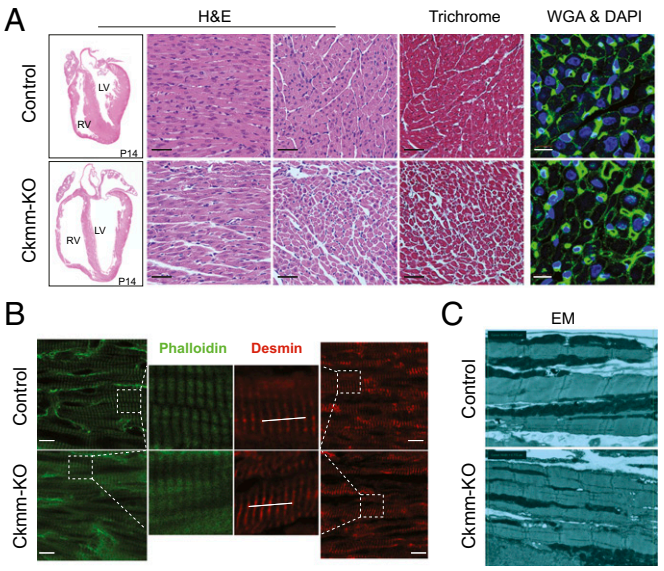

Fig. 2. Aberrant cardiomyocyte organization and contractility in *Hnrnpu* mutant hearts. (*A*) *Hnrnpu* mutant hearts are dilated and display disorganized cardiomyocytes compared with controls. Shown is the H&E staining of P14 heart sections of both control and mutant (Ckmm-KO) hearts. A low-magnification view of the heart and high-magnification views of cardiomyocyte arrangements are shown. Trichrome staining of P14 heart sections and WGA & DAPI staining for P11 heart sections are also shown. (Black scale bar, 40 μm; white scale bar in *Far Right* panels, 10 μm.) (*B*) Abnormal actin dynamics and shortened sarcomere in *Hnrnpu* mutant hearts. Heart sections (P11) were stained with phalloidin and antibodies against Desmin to reveal actin fiber and sarcomere Z line, respectively. (Scale bar, 10 μm.) (*C*) Mutant cardiomyocytes have contractility defects. Control and mutant hearts (P11) were perfused under relaxing conditions; heart sections were prepared and examined by electron microscopy. Two green lines spanning 8.772 μm were drawn in both control and mutant samples to compare the unit length of sarcomeres.

hnRNP U-deficient mice die significantly earlier than that reported for *Srsf1* mutant mice (14). We did not observe a phenotype in mice heterozygous for the *Hnrnpu* allele and carrying the *Ckmm*-Cre transgene; thus, the loss of the protein–RNA interactions, instead of the "gain-of-function" of the truncated hnRNP U protein, is responsible for the DCM phenotype.

As mentioned above, *Ckmm*-Cre is also active in skeletal muscle. To exclude the possibility that *Hnrnpu* deletion in the skeletal muscle by *Ckmm*-Cre also contributes to the observed sudden death phenotype, we crossed the conditional *Hnrnpu* knockout mice with a cardiomyocyte-specific Cre line: cardiac myosin heavy chain-α Cre (*Myh6*-Cre; its expression starts from E11.5 and continues throughout adulthood) (30). We observed a similar DCM phenotype with mutant animals generated by either *Myh6*-Cre or *Ckmm*-Cre lines. Strikingly, all of the mutant *Hnrnpu* mice generated by *Myh6*-Cre die precisely 10 d after birth. Thus, the specific loss of hnRNP U expression in cardiomyocytes is responsible for the lethal DCM phenotype. The 4-d difference of the mutant animal survival between the two Cre lines is likely due to different timing/efficiency/distribution of Cre-recombinase expression in these lines (31). Because mutant *Hnrnpu* mice generated by *Ckmm*-Cre can survive slightly longer, we exclusively used this deletion for subsequent studies.

Cardiomyocyte Disarray in hnRNP U-Deficient Hearts. Morphological alterations in *Hnrnpu* mutant hearts can be identified by H&E staining of heart sections. In control hearts, cardiomyocytes are tightly packed with scattered interstitial fibroblasts in between (Fig. 2*A*, *Top* panels). This organization is required for efficient communication and synchronized contractility of cardiomyocytes. By contrast, the distribution of cardiomyocytes in *Hnrnpu* mutant mice is markedly different. Mutant cardiomyocytes appear slightly hypertrophic and are surrounded by more white space compared with control cells (Fig. 2*A*, *Bottom*). Trichrome staining revealed an increased blue signal between cardiomyocytes in mutant hearts, suggesting increased expression of the extracellular matrix in mutant hearts (Fig. 2*A*). The overall density of cardiomyocytes is reduced in mutant hearts compared with wild type, a likely result of heart remodeling. Staining the heart sections with wheat germ agglutinin (WGA), which highlights cell membranes, reveals a pattern similar to that of the H&E staining (Fig. 2*A*, *Far Right* panels). This pattern is also observed in younger *Hnrnpu* mutant mice (P10) and becomes more obvious over time (Fig. S3).

To determine whether deletion of hnRNP U from cardiomyocytes causes cell death and contributes to heart remodeling, we stained heart sections with antibodies against cleaved Caspase 3. We detected a slight increase in apoptosis in the mutant hearts (Fig. S4 *A* and *B*). This low level of apoptosis was also reflected in Western blot analysis, as comparable levels of PARP1 protein were observed in mutant and control hearts (Fig. 1*C*). These observations indicate that hnRNP U is not required for the survival of cardiomyocytes in the early postnatal stage of development. We note that other splicing factors, including SRSF1 and SRSF2, are also not essential for cardiomyocyte survival, although they are required for embryonic development of the whole animal (14, 16).

Impaired Sarcomere Relaxation in *Hnrnpu* Mutant Heart. We next characterized the *Hnrnpu* mutant cardiomyocytes in more detail, by examining the structure of the sarcomere, the basic contracting unit in muscle cells. We carried out staining of heart sections with phalloidin and antibodies against Desmin, which reveal the actin fibers in the sarcomere and the sarcomere Z line, respectively. In control cardiomyocytes, phalloidin staining showed regular-spaced sarcomeres, with adjacent actin fibers separated by clear gaps (Fig. 2*B*). In contrast, although the pattern of sarcomere spacing was detected by phalloidin staining in mutant cells, the transition between sarcomeres is not as clear as in control cells. There are considerably higher signals in the gap between neighboring sarcomeres. In addition, the length of individual sarcomeres in *Hnrnpu* mutant cardiomyocytes appears slightly shorter; this is better revealed by Desmin staining for the sarcomere Z line. There are clearly more sarcomere units in a fixed length in mutants compared with control cells (Fig. 2*B*). These observations indicate that deletion of *Hnrnpu* in the heart adversely affects actin dynamics and sarcomere activities.

We next examined sarcomere structure by electron microscopy. Heart samples were prepared under conditions of muscle relaxation, which expose the maximal length of the sarcomere. Structural differences in the sarcomere were not observed between control and mutant samples. However, the lengths of sarcomeres and I bands were considerably reduced in mutant cardiomyocytes. As shown in Fig. 2*C* of the P11 hearts, the average length of sarcomeres (Z line to Z line) is about 2.24 μm in control samples and 1.68 μm in the *Hnrnpu* mutants. It thus appears that the ability of sarcomeres to fully relax is impaired in mutant cardiomyocytes. We also observed slightly abnormal deposition of mitochondria along sarcomeres in mutant cells, as some regions of mutant sarcomeres lacked mitochondria coverage compared with control sarcomeres (Fig. 2*C*). A decrease in mitochondria will also compromise the ability of cardiomyocytes to meet the increasing hemodynamic demand of postnatal heart development. Taken together these data indicate that loss of hnRNP U expression in cardiomyocytes results in impaired sarcomere contractility and cardiac function. These defects in conjunction with the abnormal cardiomyocyte organization observed in *Hnrnpu* mutant hearts (Fig. 2*A*) are likely to contribute significantly to heart failure.

Rapid Progression of Heart Failure in hnRNP U-Deficient Mice. To study the functional consequence of deleting *Hnrnpu* from the heart, we performed echocardiographic analysis on mutant mice, to directly monitor heart activity in vivo. Strikingly, significant cardiac dysfunction was observed in *Hnrnpu* mutant mice shortly after birth. Fig. 3*A* shows representative B- and M-mode images of the echocardiography study for P11 mutant hearts, where a dramatic increase of left ventricular anterior-to-posterior wall diameter during systole and diastole was observed. Fractional shortening (FS), which measures the strength of heart contraction, was significantly reduced in mutant hearts compared with controls (below 20% in mutants compared with above 60% in controls) (Fig. 3*B*). Examination of mutant mice from different developmental stages revealed that significantly reduced FS can be detected as early as 6 d after birth, and this decrease progresses rapidly to the time of death (Fig. 3*B*). The significantly impaired heart function in mutant mice before death correlates well with the observed abnormal histology and sarcomere activity (Fig. 2 *A*–*C*). We conclude that mice deficient in hnRNP U expression in the heart develop a severe DCM phenotype. Heart malfunction starts early after birth and progresses rapidly to cardiac failure and animal death 2 wk after birth. Remarkably, however, we did not detect a significant difference in heart rate between control and mutant mice (Fig. 3*C*), and the mutant hearts do not appear to be hypertrophic (Fig. S5).

Abnormal Calcium Handling in *Hnrnpu* Mutant Hearts. To gain additional mechanical and mechanistic insights into the failing mutant heart, we investigated the ECC activity in vivo, which is the fundamental activity of muscle cells. This was accomplished by breeding the *Hnrnpu* mutant mice with a genetically encoded calcium indicator GCaMP5 reporter line (32). In GCaMP5 reporter mice, a CAG promoter-driven GCaMP5 gene is knocked into the ROSA26 locus (32). GCaMP5 expression is normally prevented by a loxP-flanked stop cassette but can be activated by tissue-specific Cre-recombinase. Specific calcium binding by GCaMP5 protein triggers an intramolecular conformation change and emits green fluorescence upon excitation by lights of designated wavelengths (33). Calcium binding to and dissociation from GCaMP5 is concentration dependent (33), and thus, this reporter system can be used to effectively track calcium dynamics in vivo. Genetically encoded calcium indicator technology has been applied to study calcium activities in live nervous and cardiac systems with high sensitivity and resolution (32, 34). This tool can also reveal spatiotemporal details of calcium activities in *Hnrnpu* mutant hearts in vivo.

Hearts from control and mutant mice carrying the *Gcamp5* allele were imaged from the open chest under a dissecting microscope connected with a high-speed charge-coupled device (CCD) camera. Images of hearts were captured every 10 ms for multiple consecutive frames. As shown in Fig. 4*A*, GCaMP5 imaging reveals repeated calcium waves (detected by GCaMP5 fluorescence) coupled with heart contractions. The peak of calcium release (maximal brightness) is accompanied by a strong heart contraction in control hearts. The heart relaxes quickly after the level of calcium starts to decline. In control hearts, the calcium signal decreases rapidly from the peak level and continues to gradually reduce (Fig. 4*B*). A second burst of calcium release occurs at a time when the calcium level of the whole heart is barely detectable (Fig. 4*A*). New waves of calcium release and heart contraction continue after each cycle.

In contrast to control hearts, the contraction of mutant hearts is relatively weak. For example, the amplitude of mutant heart contraction is considerably reduced compared with the control heart (compare time slices 30 and 70 in both control and mutant hearts in Fig. 4*A*). This observation is consistent with the results obtained with echocardiography (Fig. 3). Careful analysis of calcium cycling and heart contraction demonstrated that mutant hearts reach the maximal calcium level slightly slower than control hearts (Fig. 4*B*; about 10 ms slower). In addition, the rate of calcium decrease in mutant hearts is considerably slower compared with controls. Calcium decays almost linearly from the peak signal in mutant hearts, in contrast to a two-phase (a rapid drop within the first 20 ms followed by a slower decrease for about 200 ms) reduction in control hearts (Fig. 4*B*). These observations revealed defects in the ECC system in *Hnrnpu* mutant hearts, with possible problems of calcium channel leakage or reduced activity of the calcium pump on the sarcoplasmic reticulum membrane. The GCaMP5 reporter line thus revealed profound heart defects caused by the loss of hnRNP U and abnormal ECC activity in mutant hearts.

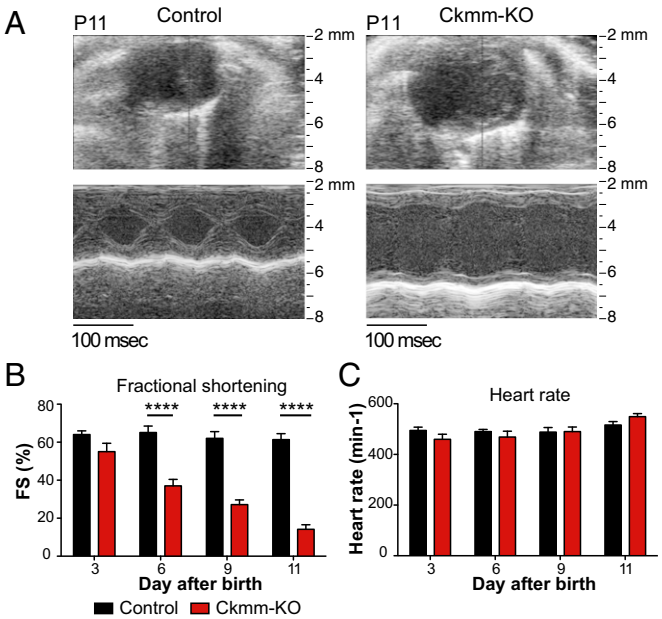

Fig. 3. Rapid heart failure in *Hnrnpu* mutant animals. (*A*) Reduced contraction strength in *Hnrnpu* mutant hearts. Shown are B- and M-mode results of echocardiography examination of control and mutant (Ckmm-KO) hearts from P11 animals. The green line in the *Upper* panel marks the position for time lapse tracing in the *Bottom* panel. (*B*) *Hnrnpu* mutant animals quickly develop severe heart malfunction. FS was calculated from echocardiography results with control and mutant animals of different ages (data were generated from eight control and six mutant mice). ****$P < 0.0001$. (*C*) *Ckmm*-Cre deletion of *Hnrnpu* from the heart has little effect on heart rates. Heart rates for control and mutant animals of different ages were recorded from echocardiograms.

Genome-Wide Gene Expression Profile in *Hnrnpu* Mutant Hearts. To gain molecular insights into the DCM phenotype caused by *Hnrnpu* deletion in the heart, we carried out RNA sequencing experiments (RNA-seq) with both control and mutant hearts from different ages (P8, P10, and P14) of the *Ckmm*-Cre deletion line (Fig. 5*A*). As expected, we observed the induction of genes frequently detected in heart failure in mutant samples from all these stages, including *Nppa*, *Nppb*, *Ctgf*, *Tgf-β* family genes, collagen genes, and stress-activated genes (*Atf4*, *Atf5*, *Asns*, etc.) (35). The top induced or repressed genes (fold change > 2) from P10 *Hnrnpu* mutant hearts are listed in Fig. 5*B*. In addition, we observed the activation of genes not previously associated with heart failure, such as the uncharacterized lncRNAs *1500017E21Rik* and *4833412C05Rik* (Fig. 5*B*). The expression of lncRNAs in the heart appears particularly sensitive to the loss of hnRNP U. As the correlation of all expressed genes between P14 control and mutant hearts is 0.941, the correlation for all lncRNAs is 0.888 (Fig. 5*C*).

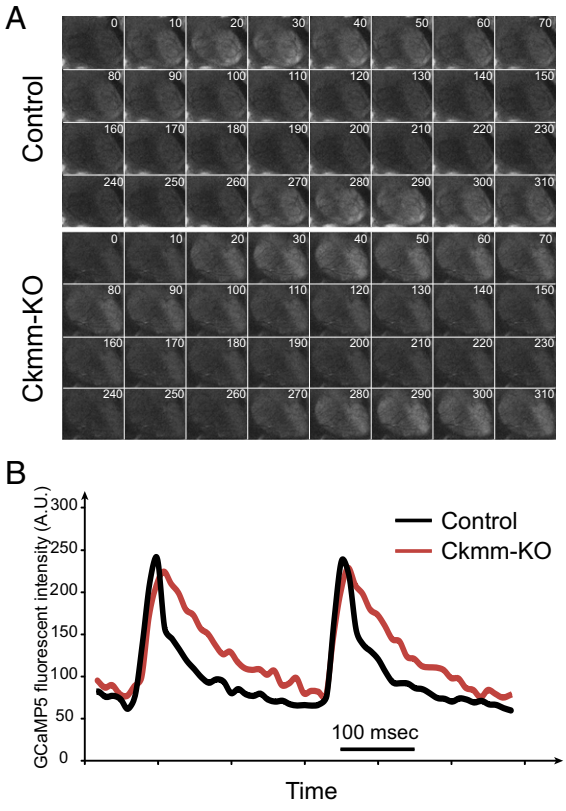

Fig. 4. *Hnrnpu* mutant hearts display abnormal calcium handling activities. (*A*) Reduced heart contractility and impaired calcium handling in *Hnrnpu* mutant hearts. Shown are a series of time lapse images of P11 control (*Top* panel) and mutant (*Bottom* panel) hearts of the GCaMP5 fluorescence. The numbers at the upper right corner in each grid indicate time (ms). (*B*) Post-contraction calcium decrease is significantly slower in *Hnrnpu* mutant hearts. The GCaMP5 fluorescence intensity over time (as shown in *A*) was quantified in ImageJ and plotted. Shown here are two consecutive calcium peaks. A.U., arbitrary unit. Similar results were obtained with six control and five mutant animals.

This observation is interesting in light of a recent report showing that lncRNA expression correlates better with human heart failure than mRNA or microRNA expression (36). We also observed expression changes of genes directly involved in ECC, including increased *Calsequestrin 1* (*Casq1*; Fig. 5*B*) and reduced *Ryr2* expression (Fig. S6 *A* and *B*) in *Hnrnpu* mutant hearts, which likely contribute to abnormal calcium activities. Gene Ontology (GO) analyses revealed an increase in secreted, extracellular matrix, cell adhesion, aminoacyl-tRNA synthetase, and amino acid transport genes in mutant hearts (Fig. S7*A*). A decrease in expression was observed for genes involved in potassium channel activity in the mutant hearts (Fig. S7*B*). Interestingly, glycoprotein and *N*-glycosylated proteins were enriched in both induced and repressed genes in the mutant, indicating dynamic regulation of glycoproteins in the mutant heart. *Hnrnpu* deletion thus appears to affect the expression and activity of multiple signal pathways in the developing heart.

Alternative Splicing in Hearts Lacking hnRNP U Expression. We determined the effect of *Hnrnpu* deletion on AS in mutant hearts from the paired-end RNA-seq data. Using the OLego program (37) and the Quantas pipeline (zhanglab.c2b2.columbia.edu/index.php/Quantas) for splicing analysis, we scored 1,234 significant AS events ($|dI| > 0.1$; Dataset S1) in *Hnrnpu* mutant hearts compared with controls (P14). These events include the use of alternative 5′ or 3′ splice sites, skipping/inclusion of single cassette exons or tandem cassette exons, intron retention, and mutual exclusion of cassette exons. The distribution of these AS events in *Hnrnpu* mutant hearts is diagrammed in Fig. 6*A*. These data show that loss of hnRNP U expression in the heart leads to extensive intron retention events (40.2%) compared with cassette skipping or inclusion (45.4%, combining both cassette and tandem cassette events; Fig. 6*A*), implicating hnRNP U in intron definition. We also observed a significant increase in skipped cassette events in *Hnrnpu* mutant hearts (77% skipping compared with 23% inclusion), suggesting that hnRNP U plays an important role in promoting exon inclusion in the heart. This observation is consistent with a previous study of hnRNP U in cultured human cells (24). These data clearly indicate that hnRNP protein family members can function to promote exon inclusion, in addition to the well-established splicing repressor activities previously proposed for hnRNP proteins, such as hnRNP A1 (1). The mixed splicing activities (skipping and inclusion) observed in *Hnrnpu* mutant hearts clearly suggest context-dependent splicing defects result from the loss of hnRNP U.

We also compared the hnRNP U splicing data obtained in this study with that obtained from studies of the effects of deleting other RBPs in the heart. A comparison of splicing changes caused by deletion of the *Rbm20* and *Rbm24* genes from the heart (11, 13) revealed that about one-third of RBM20- and RBM24-regulated exons are also regulated by hnRNP U, whereas the overlap between RBM20- and RBM24-regulated exons is minimal (Fig. 6*B*). This observation clearly demonstrates that tissue-specific splicing factors cooperate with general splicing factors to regulate the splicing of distinct groups of genes in the heart.

To gain molecular insights into *Hnrnpu* deletion-induced DCM, we examined splicing changes in specific pre-mRNAs in detail. Alternative splicing of exons 14–16 in *Camk2d* pre-mRNA (diagrammed in Fig. 6*C*), with the overexpression of the δ-A isoform (with exons 13, 15, 16, and 17 consecutively spliced), has been proposed to be a major contributing factor to the lethal DCM phenotype of *Srsf1* heart conditional knockout mice (14). We also identified this *Camk2d* alternative splicing event in the *Hnrnpu* mutant heart and confirmed this by RT-PCR (Fig. 6*C*). In addition, we detected a marked reduction of the δ-B isoform (consecutive splicing of exons 13, 14, and 17) in *Hnrnpu* mutant mice (Fig. 6*C*). These data show that like SRSF1, hnRNP U is also required to regulate alternative splicing of *Camk2d* pre-mRNA. A similar observation regarding *Camk2d* splicing has been reported in *Rbm20*-deficient rat hearts but not in the *Srsf2*-deficient mouse heart (11, 16). Because both *Rbm20* and *Srsf2* mutants also develop a DCM phenotype, these data indicate that aberrant splicing of *Camk2d* pre-mRNA is a common product of a subgroup of cardiomyopathy caused by the deletion of splicing factors.

Another example of the regulation of pre-mRNA splicing by hnRNP U is the *Titin* (*Ttn*) gene, which encodes the giant TTN protein in muscle cells (11). There are over 300 spliced exons for the *Ttn* gene, and the encoded protein product functions as a molecular spring in the sarcomere and is responsible for the passive elasticity of muscle (11). In control hearts, three major spliced isoforms are expressed from the genomic region spanning exons 112–120 (encoding the PEVK region of TTN; Fig. 6*D*). Interestingly, in *Hnrnpu* mutant cells, the number of spliced isoforms increases in this region, as multiple spliced isoforms were detected by PCR using primers spanning exons 112 and 120 (Fig. 6*D*). The loss of hnRNP U also leads to a significant reduction in the level of an isoform containing a minimal number of exons (exon 112 + 113 + 120) (Fig. 6*D*). RBM20 also regulates splicing in the same region of *Ttn* pre-mRNA (11). *Rbm20* mutant cells express higher MW TTN proteins, which might contribute to the cardiomyopathy phenotype in the *Rbm20* mutant rat. It is striking that multiple RBPs (hnRNP U, SRSF1, RBM20) all regulate the splicing of the same target genes (*Camk2d* and *Ttn*). Generation of the correct pre-mRNA splicing pattern requires the coordinated activities of both general and tissue-specific splicing factors.

Further analysis of the RNA-seq data revealed many additional splicing targets of hnRNP U, including *Camk2g*, *Pstk*, and

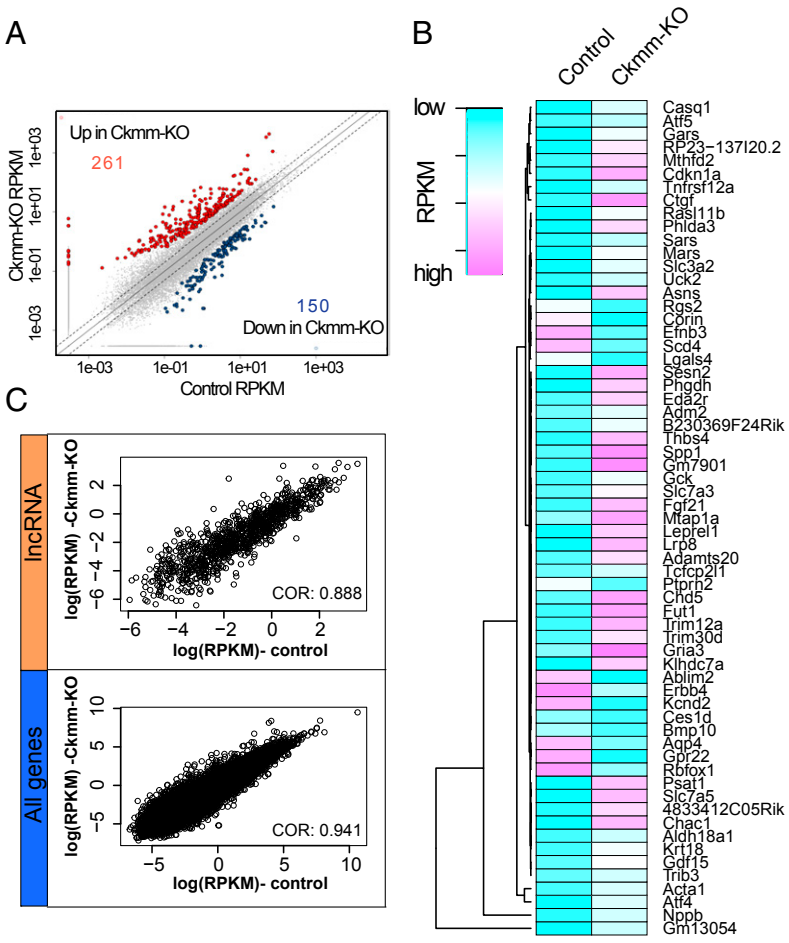

Fig. 5. Deletion of *Hnrnpu* from the heart moderately affects the gene expression program. (*A*) Whole genome expression profile of *Hnrnpu* mutant hearts. RNA was extracted from control and mutant hearts and subjected to RNA-seq analysis. A two-way plot is shown. Genes whose expression levels are significantly induced or repressed in P14 mutant hearts are labeled in the upper left and bottom right of the panel, respectively. RPKM, reads per kilobase per million mapped reads. (*B*) A heat map list of top induced or repressed genes in *Hnrnpu* mutant hearts. (*C*) *Hnrnpu* deletion has strong effects on lncRNA expression in the heart. Shown are correlations (COR) of the expression of all lncRNAs (*Top*) or total genes (*Bottom*) between control and mutant hearts determined from P14 RNA-seq data.

Junctin pre-mRNAs. Loss of hnRNP U expression leads to the exclusion of exon 14 in *Camk2g* pre-mRNA (Fig. 6*E*) and the inclusion of exon 2 in *Pstk* (Fig. 6*F*) and exon 3 in *Junctin* pre-mRNAs (Fig. 6*G*). We also confirmed the expression change of the lncRNA *4833412C05Rik* (renamed *Bigheart*) in *Hnrnpu* mutant hearts (Fig. 6*H*). Interestingly, Bigheart is expressed as two alternatively spliced isoforms in *Hnrnpu* mutant cells (Fig. 6*H*). Kinetic studies with control and mutant mice of different ages (P1, P4, P8, and P14) revealed an interesting pattern of expression of *Bigheart* in postnatal heart development. This RNA is expressed at relatively high levels in newborn mice but decreases dramatically after 1 wk (Fig. 6*I*). However, deletion of hnRNP U leads to the persistent expression of *Bigheart* in the heart, and the accumulation of an alternatively spliced *Bigheart* isoform with an internal exon 2 skipped. We note that the induction of *Bigheart* occurs in a number of heart failure models [e.g., transverse aortic constriction (TAC)- and myocardial infarction (MI)-induced heart failure models; Fig. S8], but the aberrant splicing of *Bigheart* pre-mRNA appears to be specific to the *Hnrnpu* mutant mice. Because altered splicing of *Bigheart*, *Ttn*, *Pstk*, *Junctin*, *Camk2d*, and *Camk2g* can all be detected at relatively early stages of development in *Hnrnpu* mutant hearts (Fig. 6*I*), the alternative splicing of these pre-mRNAs is likely to be directly regulated by hnRNP U during postnatal heart development, rather than the consequences of heart failure. Consistent with this, no significant changes of alternative splicing of these genes can be detected in TAC and MI mouse heart failure samples (Fig. S8).

In summary, we observed alternative splicing events in *Hnrnpu* mutant hearts that have previously been implicated in cardiomyopathy; we also identified splicing events that are specifically regulated by hnRNP U in the heart. It is clear that *Hnrnpu* deletion in cardiomyocytes causes many misregulated events and results in multiple defects in the heart. These defects collectively lead to a severe lethal DCM phenotype in mutant mice.

An Alternatively Spliced Junctin Protein Isoform Is *N*-Glycosylated. *Junctin* encodes an ECC component on the sarcoplasmic reticulum membrane and is required for normal ECC activity (38). The increased ECC activity and contractility during postnatal heart development correlate with increased Junctin expression in both human and mouse hearts (39, 40) (also see Fig. S1). Significantly, reduced expression of Junctin protein has been reported in human heart failure patients (41). In addition, transgenic mice overexpressing Junctin in the heart display impaired relaxation and aberrant calcium handling (42). Finally, mice deficient for Junctin show sarcoplasmic reticulum calcium overloading defects and altered cardiac contractility (39). *Junctin* alternative splicing (the same

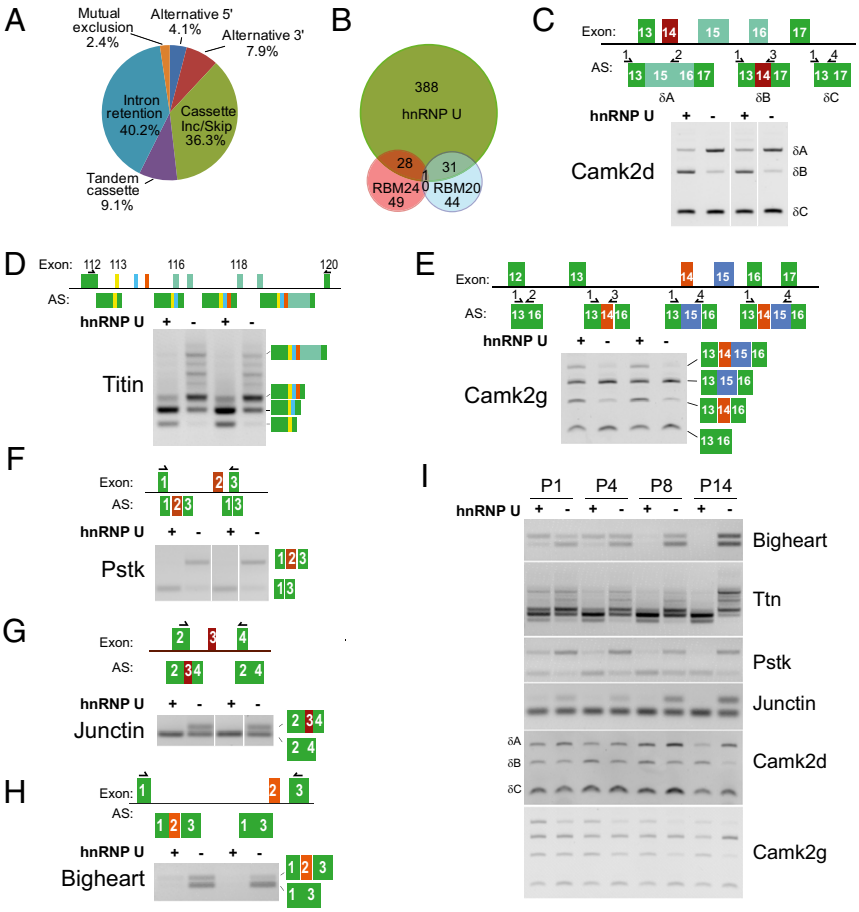

Fig. 6. *Hnrnpu* deletion affects AS in the heart. (*A*) Distribution of various alternative splicing events in *Hnrnpu* mutant hearts. Calculations were conducted with the total 1,234 scored events from the P14 data. (*B*) hnRNP U coregulates the splicing of a distinct subgroup of pre-mRNAs with RBM20 and RBM24 in the heart. hnRNP U-regulated cassette RNA splicing events were analyzed together with published RBM20 and RBM24 exon splicing events. The overlaps between each of the datasets are diagramed. (*C*) hnRNP U regulates alternative splicing of exons 14–16 of the *Camk2d* pre-mRNA. The exon position, various alternative splicing products, and RT-PCR primer positions are diagramed. Plus and minus signs above the gel picture indicate control and mutant samples, respectively. (*D*) *Ttn* pre-mRNA splicing is regulated by hnRNP U. (*E–H*) Examples of additional splicing targets of hnRNP U: *Camk2g* (*E*), *Pstk* (*F*), *Junctin* (*G*), and *Bigheart* (*H*). (*I*) Time course of splicing changes of selected genes in *Hnrnpu* mutant hearts. RT-PCR was conducted with P1, P4, P8, and P14 heart samples using primers designed for the detection of specific splicing products. Some lanes in *C*, *F*, and *G* were spliced and rearranged from the same gels to keep a consistent loading order.

cassette event as we identified here; Figs. 6*G* and 7*A*) was reported in human samples (43), but its function and potential link to heart failure is not known. We therefore decided to study the alternative splicing of Junctin in more detail.

First, we confirmed that the alternatively spliced Junctin (JAS) protein isoform is expressed in *Hnrnpu* mutant hearts. Using antibodies specific for Junctin protein, we detected a band in *Hnrnpu* mutant hearts in addition to the normal Junctin protein by Western blotting (Fig. 7*B*). Surprisingly, the hnRNP U-specific band migrates slower than expected for a protein containing just 15 additional amino acids (encoded by the 45 bp alternatively spliced exon) compared with the normal Junctin (JCT) protein. It therefore seemed likely that the JCT protein encoded by JAS pre-mRNA is posttranslationally modified. The alternatively spliced exon 3 is highly conserved across evolution (Fig. 7*A*), and motif analysis by NetNGlyc algorithm (www.cbs.dtu.dk/services/NetNGlyc/) predicted that the asparagine residue at position 64 (N64, within the full-length JAS protein) is likely to be *N*-glycosylated, as it is contained within the consensus sequence (*N*-X-S/T) for this posttranslational modification. To test this possibility, we cloned cDNAs encoding JCT and JAS from *Hnrnpu* mutant hearts and expressed them in 293T cells. We found that JAS migrates as two bands in SDS/PAGE (Fig. 7*C*), with one band slightly slower than JCT, corresponding to unmodified JAS (contains 15 more amino acids than JCT). The other slower band migrates to a similar position as the additional Junctin band detected in *Hnrnpu* mutant hearts. To determine whether this JAS protein isoform is indeed *N*-glycosylated at N64, we carried out two lines of experiments. First, we introduced a number of point mutations into the JAS expression construct. Strikingly, the slower migrating band was abolished by mutating the N64 residue to encode isoleucine (N64I) or glutamine (N64Q), whereas mutating an adjacent leucine 65 to isoleucine (L65I) had no effect (Fig. 7*C*). These experiments demonstrate that N64 is required for the modification. In addition, we showed that PNGase F, an enzyme that specifically removes *N*-glycosylated polysaccharides from modified proteins, specifically removed the modification from JAS (Fig. 7*D*). Taken together, these data show that Junctin protein generated by AS is, indeed, *N*-glycosylated at amino acid N64.

To investigate whether JAS interacts with different proteins and potentially contributes to different physiological properties in cardiomyocytes, we made use of the mouse cardiomyocyte cell line HL-1. We generated stable HL-1 cells that overexpressed Junctin, JAS, or JAS N64I by infecting parental cells with lentiviruses encoding these proteins. JCT, JAS, and JAS N64I proteins

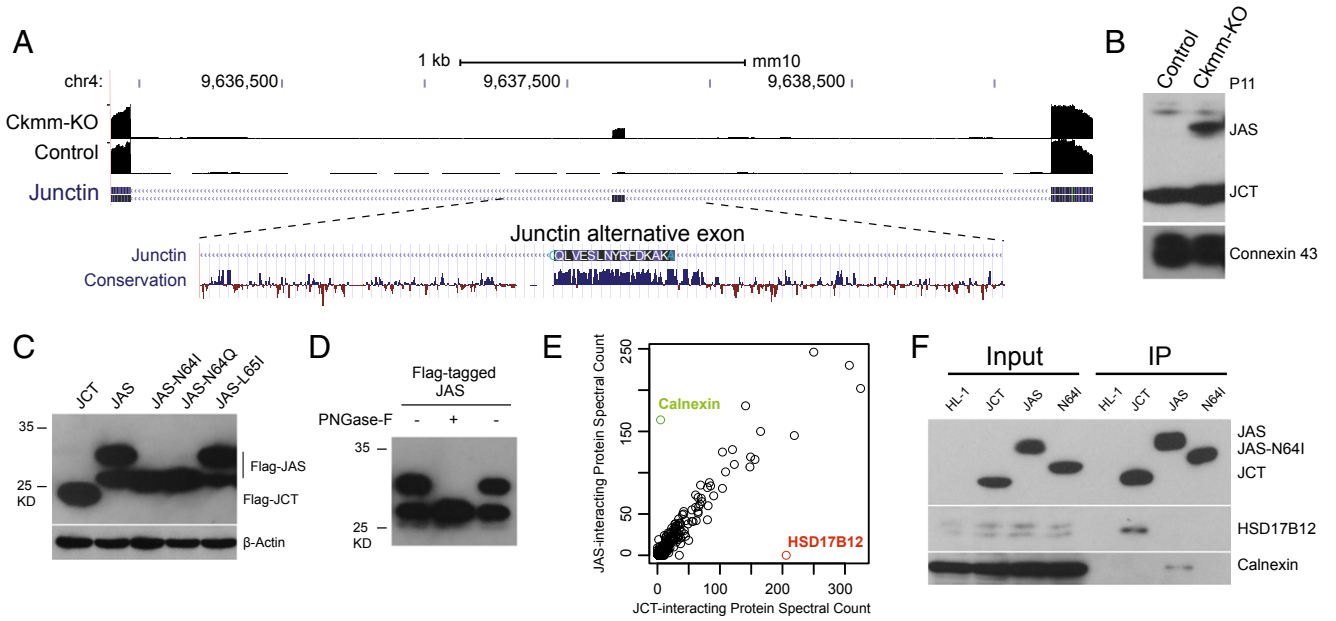

Fig. 7. Alternatively spliced Junctin isoform is *N*-glycosylated. (*A*) The alternatively spliced exon of the *Junctin* pre-mRNA is conserved. Shown are RNA-seq reads from both control and *Hnrnpu* mutant hearts aligned to the Junctin exons 2–4 region. A conservation graph from the UCSC genome browser is also shown under the gene track. (*B*) Expression of the alternatively spliced Junctin isoform in *Hnrnpu* mutant hearts. Protein lysates from both control and mutant hearts (P11) were prepared and subjected to Western blot analysis for Junctin and Connexin 43 expression. (*C*) JAS is modified at N64. Flag-tagged JCT, JAS, and various point mutations of JAS expression constructs were transfected into 293T cells and protein lysates were prepared for the analysis of the tagged JCT, JAS, and β-Actin expression by Western blotting. (*D*) JAS modification is *N*-glycosylation. JAS proteins overexpressed in 293T cells were immunoprecipitated using anti-Flag beads and treated with PNGase F, and the elimination of the slow migrating band was revealed by Western blotting. (*E*) JCT and JAS interact with distinct proteins. Stable HL-1 cells expressing JCT or JAS were generated by infecting parental cells with a lentivirus encoding these proteins. Flag immunoprecipitation was conducted to pull down proteins that interact with JCT and JAS and analyzed by mass spectrometry. Spectral counts of interacting proteins with JCT and JAS were plotted against each other. (*F*) Verification of a subset of interactors identified by MS experiments. Protein lysates from various HL-1 stable clones and their respective immunoprecipitation products were analyzed by Western blotting for interactions between HSD17b12 and Calnexin with JCT and JAS.

were Flag-tagged at the C terminus and expressed at a comparable level. Interestingly, all of the JAS proteins expressed in HL-1 cells are *N*-glycosylated (Fig. 7*F*). We conducted immunoprecipitation experiments using antibodies against Flag to pull down proteins that interact with Junctin splicing variants. Mass spectrometry experiments were subsequently conducted to identify proteins that commonly or uniquely interact with Junctin or JAS. We found that there are many sarcoplasmic reticulum and ribosomal proteins that interact with both JCT and JAS (Dataset S2). Strikingly, Calnexin and HSD17b12, which are known endoplasmic reticulum membrane proteins (44, 45), specifically interact with JAS and JCT, respectively (Fig. 7*E*). We confirmed these interactions with corresponding Junctin splicing variants by Western blot (Fig. 7*F*). These data clearly demonstrate distinct biochemical properties of Junctin splicing variants generated by the loss of hnRNP U.

Discussion

The hnRNP U protein has been implicated in many levels of gene regulation, including the maintenance of intranuclear chromosome conformation, and in transcription, RNA splicing, and DNA repair (19, 21, 46, 47). The generation of the *Hnrnpu* conditional deletion allele provided the opportunity to study the function of hnRNP U in vivo, in specific tissues. In particular, we chose the heart, as the development and function of the mouse heart has proven to be a sensitive indicator of defects in RNA metabolism (14, 16). Here we demonstrate that hnRNP U is required for normal gene expression and postnatal heart development and function. Conditional deletion of *Hnrnpu* in the mouse heart leads to death around 2 wk after birth due to severe DCM.

The cardiac contraction system is at the center of heart development and function, and proper developmental regulation of the expression and RNA splicing of ECC and sarcomere components is required for normal heart function (6). Diverse functions of splicing variants appear to have evolved for this purpose. For example, the expression of many heart proteins is regulated at the level of splicing, which appears to be necessary for the correct subcellular localization, protein modification, and enzymatic activities of heart proteins (7). The function of the ECC and sarcomere is sensitive to the aberrant expression of structural components or altered cellular environments, and changes of ECC and sarcomere contraction lead to heart malfunction and disease (48). A number of splicing factors have been shown to be required for normal heart development and function (11, 13–16). They include both general and tissue-specific splicing factors.

Development of the embryonic heart appears not to be affected by the deletion of the *Hnrnpu* gene, as both *Ckmm*-Cre and *Myh6*-Cre deletion lines give rise to live mutant pups with no apparent defects. Similar observations were made in both *Srsf1* and *Srsf2* conditional knockout mice (14, 16). However, postnatal heart development and function require an intact RNA splicing program, as both *Hnrnpu* and *Srsf1* mutant mice die a few weeks after birth due to postnatal heart failure. A recent report showed that postnatal heart development is accompanied by major splicing changes (6). We have shown that hnRNP U plays a major role in the normal regulation of RNA splicing in the postnatal heart. The impact of this abnormal splicing is striking, as multiple defects were observed in *Hnrnpu* mutant hearts, including aberrant cardiomyocyte arrangement, impaired calcium handling, and contractility. These defects collectively contribute to the severe DCM phenotype in *Hnrnpu* mutant mice.

Coordination of RNA Splicing by hnRNP and Other RBPs. Analyses of splicing changes in *Hnrnpu* mutant hearts showed that splicing targets are either hnRNP U-specific or shared among selected splicing factors. *Camk2d* is one example of pre-mRNAs that are regulated by multiple factors, including SRSF1, RBM20, and hnRNP U. *Ttn* alternative splicing is also regulated by both hnRNP U and RBM20. For many hnRNP U-specific splicing targets—for example, *Pstk* and *Junctin*—it is likely that their splicing also requires the concerted activities of other RBPs. Proper splicing requires coordination of the activities of both general and tissue-specific splicing factors. Remarkably, RBM20 and RBM24, both muscle-specific splicing factors, regulate mostly nonoverlapping splicing targets. However, ∼30% of RBM20 and RBM24 splicing targets are also regulated by hnRNP U. In general, it appears that the activities of tissue-specific and general splicing factors function together to regulate the alternative splicing of specific sets of target pre-mRNAs. The splicing identity of a specific tissue is determined by the combined activities of distinct splicing complexes formed on different groups of pre-mRNAs. It is important to point out that splicing factors can regulate AS directly through protein–RNA interactions or indirectly through affecting the expression of other RBPs. Examination of the relationship between specific RBP–RNA interactions in the presence or absence of other splicing factors coupled with subsequent splicing outcomes should provide interesting insights into the mechanisms by which distinct splicing factors function together to regulate splicing.

Alternative Splicing of ECC Components and Protein Glycosylation. Many components of the ECC machinery are subjected to splicing regulation during development or under disease conditions (7). Alternative splicing of *Ryr2*, *Triadin*, and *Atp2a2* has been reported (7), and protein products of splicing variants affect calcium handling in myocytes in general. We show here that hnRNP U specifically regulates alternative splicing of *Junctin* pre-mRNA, as the deletion of *Hnrnpu* leads to an aberrant splicing product of Junctin. The JAS protein is *N*-glycosylated at a specific asparagine site (N64). JAS glycosylation occurs at the luminal side of the sarcoplasmic reticulum; thus, glycosylation could potentially affect the interactions between Junctin and other sarcoplasmic reticulum proteins. We showed that *N*-glycosylated JAS is specifically recognized by Calnexin, and it disrupts the normal interactions between JCT and HSD17B12. The interaction between glycosylated JAS and Calnexin is not surprising, as Calnexin plays an important role in glycoprotein folding and maturation (49). It could also potentially lead to different turnover rates of Junctin splicing variants and thus affect calcium dynamics in cardiomyocytes. We also identified an interesting interaction partner, HSD17B12, for Junctin in this study. HSD17B12 is highly expressed in neural tissues as well as in the heart, and it is required for mouse embryonic organogenesis (50). HSD17B12 is an ER membrane protein known to play an important role in steroid and fat metabolism (44, 51). The interaction between Junctin and HSD17B12 (Fig. 7 *E* and *F*) suggests a possible coupling between lipid metabolism and calcium handling in cardiomyocytes.

It is interesting to note that about half of the Triadin proteins are also *N*-glycosylated at a specific asparagine site (N75) in the heart (52). Glycosylation of Triadin appears to increase its stability (53) and possibly other functions. Glycosylation is also known to occur during the maturation of the sarcoplasmic reticulum calcium-binding protein Calsequestrin, and altered Calsequestrin glycosylation has been linked to heart failure in canine models of heart diseases (54). Thus, it appears that glycosylation is an important regulatory mechanism in cardiomyocyte physiology. Further studies are required to determine the physiological function of JAS glycosylation and its potential contribution to heart physiology. However, the hnRNP U-dependent alternative RNA splicing of *Junctin* pre-mRNA provides an interesting example of the role of splicing regulation in controlling the modification and function of proteins.

Materials and Methods

Mouse Strains. The generation of *Hnrnpu* conditional deletion allele is described in detail in *SI Materials and Methods*. All animal experimental procedures were in accordance with protocols approved by the Institutional Animal Care and Use Committees of Columbia University Medical Center.

Histology, Immunofluorescence Staining, and Electron Microscopy. Mouse hearts from animals of different ages were dissected and fixed with 4% (wt/vol) formaldehyde. H&E and trichrome stainings were conducted according to standard procedures with paraffin-embedded heart sections. Immunofluorescence staining was performed with heart sections prepared by Leica vibratome with agarose embedding. Electron microscopy analysis of hearts was conducted by the conventional osmium–uranium–lead method, with heart samples perfused first with a heparin-containing Krebs–Henseleit Buffer (10 U/mL heparin in 118 mM NaCl, 4.7 mM KCl, 1.2 mM KH_2PO_4, 1.2 mM $MgSO_4$, 25 mM $NaHCO_3$, 11 mM Glucose) and followed by standard procedures. Images were acquired by Zeiss SIGMA Field Emission Scanning Electron Microscope. The average length of the sarcomere (Z line to Z line) was determined from at least 20 units.

RNA-Seq for Expression and Splicing Analysis. Total RNA from dissected control and mutant hearts was isolated by TRIzol reagent (Invitrogen). The sequencing library was prepared with the Nextera sample preparation kit (Illumina) and subjected to HiSEQ paired-end 100 bp plus sequencing. ExpressionPlot (55) pipeline was used for expression analysis; OLego (37) and Quantas pipelines were used for alternative splicing analysis.

Cell Culture, Molecular Cloning, Transfection, Western Blot, and Lentivirus Infection. These assays were performed according to routine procedures. Please refer to *SI Materials and Methods* for details.

ACKNOWLEDGMENTS. We thank Wei Tan for performing TAC and MI surgeries. We also thank members of the T.M. laboratory for discussions and comments on the manuscript. This work was supported by US National Institutes of Health (NIH) Pioneer Grant 8DP1NS082099 (to T.M.) and startup funds from the Columbia University Medical Center. E.N.O. was supported by NIH Grants HL-077439, HL-111665, HL-093039, DK-099653, and U01-HL-100401; the Foundation Leducq Networks of Excellence; the Cancer Prevention and Research Institute of Texas; and Robert A. Welch Foundation Grant 1-0025. N.B. was supported by a Marie Curie International Outgoing Fellowship within the 7th European Community Framework Program.

1. Black DL (2003) Mechanisms of alternative pre-messenger RNA splicing. *Annu Rev Biochem* 72:291–336.
2. Maniatis T, Tasic B (2002) Alternative pre-mRNA splicing and proteome expansion in metazoans. *Nature* 418(6894):236–243.
3. Grabowski PJ, Black DL (2001) Alternative RNA splicing in the nervous system. *Prog Neurobiol* 65(3):289–308.
4. Wang GS, Cooper TA (2007) Splicing in disease: Disruption of the splicing code and the decoding machinery. *Nat Rev Genet* 8(10):749–761.
5. Fu XD, Ares M, Jr (2014) Context-dependent control of alternative splicing by RNA-binding proteins. *Nat Rev Genet* 15(10):689–701.
6. Giudice J, et al. (2014) Alternative splicing regulates vesicular trafficking genes in cardiomyocytes during postnatal heart development. *Nat Commun* 5:3603.
7. Lara-Pezzi E, Gómez-Salinero J, Gatto A, García-Pavía P (2013) The alternative heart: Impact of alternative splicing in heart disease. *J Cardiovasc Transl Res* 6(6):945–955.
8. Giudice J, Cooper TA (2014) RNA-binding proteins in heart development. *Adv Exp Med Biol* 825:389–429.
9. Lambert N, et al. (2014) RNA Bind-n-Seq: Quantitative assessment of the sequence and structural binding specificity of RNA binding proteins. *Mol Cell* 54(5):887–900.
10. Yeo GW, et al. (2009) An RNA code for the FOX2 splicing regulator revealed by mapping RNA-protein interactions in stem cells. *Nat Struct Mol Biol* 16(2):130–137.
11. Guo W, et al. (2012) RBM20, a gene for hereditary cardiomyopathy, regulates titin splicing. *Nat Med* 18(5):766–773.
12. Maatz H, et al. (2014) RNA-binding protein RBM20 represses splicing to orchestrate cardiac pre-mRNA processing. *J Clin Invest* 124(8):3419–3430.
13. Yang J, et al. (2014) RBM24 is a major regulator of muscle-specific alternative splicing. *Dev Cell* 31(1):87–99.
14. Xu X, et al. (2005) ASF/SF2-regulated CaMKIIdelta alternative splicing temporally reprograms excitation-contraction coupling in cardiac muscle. *Cell* 120(1):59–72.
15. Feng Y, et al. (2009) SRp38 regulates alternative splicing and is required for Ca(2+) handling in the embryonic heart. *Dev Cell* 16(4):528–538.
16. Ding JH, et al. (2004) Dilated cardiomyopathy caused by tissue-specific ablation of SC35 in the heart. *EMBO J* 23(4):885–896.

17. Dreyfuss G, Matunis MJ, Piñol-Roma S, Burd CG (1993) hnRNP proteins and the biogenesis of mRNA. *Annu Rev Biochem* 62:289–321.
18. Kamma H, Portman DS, Dreyfuss G (1995) Cell type-specific expression of hnRNP proteins. *Exp Cell Res* 221(1):187–196.
19. Kukalev A, Nord Y, Palmberg C, Bergman T, Percipalle P (2005) Actin and hnRNP U cooperate for productive transcription by RNA polymerase II. *Nat Struct Mol Biol* 12(3):238–244.
20. Romig H, Fackelmayer FO, Renz A, Ramsperger U, Richter A (1992) Characterization of SAF-A, a novel nuclear DNA binding protein from HeLa cells with high affinity for nuclear matrix/scaffold attachment DNA elements. *EMBO J* 11(9):3431–3440.
21. Hasegawa Y, et al. (2010) The matrix protein hnRNP U is required for chromosomal localization of Xist RNA. *Dev Cell* 19(3):469–476.
22. Hacisuleyman E, et al. (2014) Topological organization of multichromosomal regions by the long intergenic noncoding RNA Firre. *Nat Struct Mol Biol* 21(2):198–206.
23. Xiao R, et al. (2012) Nuclear matrix factor hnRNP U/SAF-A exerts a global control of alternative splicing by regulating U2 snRNP maturation. *Mol Cell* 45(5):656–668.
24. Huelga SC, et al. (2012) Integrative genome-wide analysis reveals cooperative regulation of alternative splicing by hnRNP proteins. *Cell Reports* 1(2):167–178.
25. Kiledjian M, Dreyfuss G (1992) Primary structure and binding activity of the hnRNP U protein: Binding RNA through RGG box. *EMBO J* 11(7):2655–2664.
26. Roshon MJ, Ruley HE (2005) Hypomorphic mutation in hnRNP U results in post-implantation lethality. *Transgenic Res* 14(2):179–192.
27. Brüning JC, et al. (1998) A muscle-specific insulin receptor knockout exhibits features of the metabolic syndrome of NIDDM without altering glucose tolerance. *Mol Cell* 2(5):559–569.
28. Göhring F, Schwab BL, Nicotera P, Leist M, Fackelmayer FO (1997) The novel SAR-binding domain of scaffold attachment factor A (SAF-A) is a target in apoptotic nuclear breakdown. *EMBO J* 16(24):7361–7371.
29. Seidman JG, Seidman C (2001) The genetic basis for cardiomyopathy: From mutation identification to mechanistic paradigms. *Cell* 104(4):557–567.
30. Gaussin V, et al. (2002) Endocardial cushion and myocardial defects after cardiac myocyte-specific conditional deletion of the bone morphogenetic protein receptor ALK3. *Proc Natl Acad Sci USA* 99(5):2878–2883.
31. Davis J, Maillet M, Miano JM, Molkentin JD (2012) Lost in transgenesis: A user's guide for genetically manipulating the mouse in cardiac research. *Circ Res* 111(6):761–777.
32. Zariwala HA, et al. (2012) A Cre-dependent GCaMP3 reporter mouse for neuronal imaging in vivo. *J Neurosci* 32(9):3131–3141.
33. Nakai J, Ohkura M, Imoto K (2001) A high signal-to-noise Ca(2+) probe composed of a single green fluorescent protein. *Nat Biotechnol* 19(2):137–141.
34. Tallini YN, et al. (2006) Imaging cellular signals in the heart in vivo: Cardiac expression of the high-signal Ca2+ indicator GCaMP2. *Proc Natl Acad Sci USA* 103(12):4753–4758.
35. Frey N, Olson EN (2003) Cardiac hypertrophy: The good, the bad, and the ugly. *Annu Rev Physiol* 65:45–79.
36. Yang KC, et al. (2014) Deep RNA sequencing reveals dynamic regulation of myocardial noncoding RNAs in failing human heart and remodeling with mechanical circulatory support. *Circulation* 129(9):1009–1021.
37. Wu J, Anczuków O, Krainer AR, Zhang MQ, Zhang C (2013) OLego: Fast and sensitive mapping of spliced mRNA-Seq reads using small seeds. *Nucleic Acids Res* 41(10):5149–5163.
38. Fan GC, Yuan Q, Kranias EG (2008) Regulatory roles of junctin in sarcoplasmic reticulum calcium cycling and myocardial function. *Trends Cardiovasc Med* 18(1):1–5.
39. Yuan Q, et al. (2007) Sarcoplasmic reticulum calcium overloading in junctin deficiency enhances cardiac contractility but increases ventricular automaticity. *Circulation* 115(3):300–309.
40. Jung DH, Lee CJ, Suh CK, You HJ, Kim DH (2005) Molecular properties of excitation-contraction coupling proteins in infant and adult human heart tissues. *Mol Cells* 20(1):51–56.
41. Gergs U, et al. (2007) On the role of junctin in cardiac Ca2+ handling, contractility, and heart failure. *Am J Physiol Heart Circ Physiol* 293(1):H728–H734.
42. Kirchhefer U, et al. (2003) Impaired relaxation in transgenic mice overexpressing junctin. *Cardiovasc Res* 59(2):369–379.
43. Lim KY, Hong CS, Kim DH (2000) cDNA cloning and characterization of human cardiac junctin. *Gene* 255(1):35–42.
44. Moon YA, Horton JD (2003) Identification of two mammalian reductases involved in the two-carbon fatty acyl elongation cascade. *J Biol Chem* 278(9):7335–7343.
45. Wada I, et al. (1991) SSR alpha and associated calnexin are major calcium binding proteins of the endoplasmic reticulum membrane. *J Biol Chem* 266(29):19599–19610.
46. Göhring F, Fackelmayer FO (1997) The scaffold/matrix attachment region binding protein hnRNP-U (SAF-A) is directly bound to chromosomal DNA in vivo: A chemical cross-linking study. *Biochemistry* 36(27):8276–8283.
47. Hegde ML, et al. (2012) Enhancement of NEIL1 protein-initiated oxidized DNA base excision repair by heterogeneous nuclear ribonucleoprotein U (hnRNP-U) via direct interaction. *J Biol Chem* 287(41):34202–34211.
48. Harvey PA, Leinwand LA (2011) The cell biology of disease: Cellular mechanisms of cardiomyopathy. *J Cell Biol* 194(3):355–365.
49. Helenius A, Aebi M (2004) Roles of N-linked glycans in the endoplasmic reticulum. *Annu Rev Biochem* 73:1019–1049.
50. Rantakari P, et al. (2010) Hydroxysteroid (17beta) dehydrogenase 12 is essential for mouse organogenesis and embryonic survival. *Endocrinology* 151(4):1893–1901.
51. Luu-The V, Tremblay P, Labrie F (2006) Characterization of type 12 17beta-hydroxysteroid dehydrogenase, an isoform of type 3 17beta-hydroxysteroid dehydrogenase responsible for estradiol formation in women. *Mol Endocrinol* 20(2):437–443.
52. Kobayashi YM, Jones LR (1999) Identification of triadin 1 as the predominant triadin isoform expressed in mammalian myocardium. *J Biol Chem* 274(40):28660–28668.
53. Milstein ML, McFarland TP, Marsh JD, Cala SE (2008) Inefficient glycosylation leads to high steady-state levels of actively degrading cardiac triadin-1. *J Biol Chem* 283(4):1929–1935.
54. Jacob S, et al. (2013) Altered calsequestrin glycan processing is common to diverse models of canine heart failure. *Mol Cell Biochem* 377(1-2):11–21.
55. Friedman BA, Maniatis T (2011) ExpressionPlot: A web-based framework for analysis of RNA-Seq and microarray gene expression data. *Genome Biol* 12(7):R69.
56. Garg A, et al. (2014) KLHL40 deficiency destabilizes thin filament proteins and promotes nemaline myopathy. *J Clin Invest* 124(8):3529–3539.